Chapter 5

Asymmetric reactions as a probe for density dependence of symmetry energy in intermediate energy heavy-ion collisions: A detailed investigation

5.1 Introduction

As stated earlier in this thesis, with the continuous advancements in the radioactive ion beam facilities (RIBs) at several laboratories around the world, experimental studies involving neutron-rich nuclei have set an excellent platform to investigate the isospin dependence in the dynamics of heavy-ion collisions at intermediate energies. It has also opened up a new field that helps in extracting the knowledge about the equation of state of asymmetric nuclear matter, a topic of current debate. It is now well accepted that the isospin effects come into picture via symmetry energy and isospin-dependent binary nucleon-nucleon cross-section. Though, considerable success has been achieved in narrowing down the magnitude and form of the binary isospin-dependent nucleon-nucleon cross-section, the density dependence of symmetry energy is far from being settled down. This probably happened due to dual dependence of most of the observables on both.

The knowledge about the nuclear symmetry energy as well as its density dependence helps in understanding not only the gross characteristics of nuclear matter but, also various astrophysical phenomena [46]. A lot of efforts have been made to constraint the density dependence of nuclear symmetry energy, both at sub-saturation and supra-saturation

density regions with the help of variety of observables [46, 126, 181, 235, 284, 317–331]. Unfortunately, theoretical calculations failed to predict the precise density dependence of the symmetry energy [332–334].

One generally discusses either sub-saturation or supra-saturation density region. The behavior of nuclear symmetry energy at sub-saturation density region has been constrained up to certain extent by studying the observables such as isospin diffusion [46, 126, 181, 317], isospin fractionation [322], isobaric ratios of various species [46, 323], fragment yields, single and double neutron-proton (n-p) ratios [46, 318–320, 324], photon production [46, 325] etc. On the other side, observables like π^-/π^+ ratio [46, 326], the n-p differential collective flow [46, 284, 327], triton/He^3 ratio [46, 328], K^+/K^0 ratio [46, 329], η meson production [46, 330] etc. can be used to probe the high density (i.e., at supra-saturation density region) behavior of symmetry energy. In the coming sections, we will first review some of the efforts made in the past to constrain the density dependence of symmetry energy both at sub-saturation and supra-saturation density regions with the help of observables listed above. It is also worth mentioning that in addition to above listed reaction observables, nuclear structure studies such as neutron skin [46, 335], giant and pygmy dipole resonances [46, 336] etc. have also been reported as observables to probe (and constrain) the density dependence of symmetry energy.

5.2 Density dependence of symmetry energy

The energy per particle of an asymmetric nuclear matter w.r.t. density ρ and an isospin asymmetry $\delta_{\acute{A}} = (\rho_n - \rho_p)$, can be determined by the parabolic law [46, 337], i.e.,

$$E_{sym}(\rho, \delta_{\acute{A}}) = E_{sym}(\rho, 0) + E_{sym}(\rho)\delta^2_{\acute{A}}, \tag{5.1}$$

where, $E_{sym}(\rho,0)$ and $E_{sym}(\rho)$ represent the energy per particle of symmetric nuclear matter and the nuclear symmetry energy, respectively. As one moves away from the normal nuclear matter density and β-stability line, the understanding of the density dependence of symmetry energy weakens [46, 337]. Therefore, in such a situation, the equation given below provides the parametrization for the density dependence of symmetry energy:

$$E_{sym}(\rho) = E_{sym}(\rho_0)\left(\frac{\rho}{\rho_0}\right)^{\gamma'}. \tag{5.2}$$

The parameter γ' (see Eq. 5.2) determines the stiffness of the symmetry energy at densities away from the saturation density. The strength of the symmetry energy is different for

different values of γ'. A lot of research is going on to constrain (and probe) the symmetry energy with the help of various observables. Generally, two different forms of density dependence of symmetry energy have been advocated:

- soft density dependence: here, symmetry energy increases up to normal nuclear matter density and then decreases afterwards at high densities and;
- stiff density dependence: here, symmetry energy tends to increase monotonically with the density.

During the past few years, a lot of work has been done to extract the strength of symmetry energy as well as its density dependence. The stiff symmetry energy will result in a larger neutron skin thickness and can lead to larger neutron star radii and rapid cooling of the neutron star [338–340]. Moreover, thorough survey of the literature suggests different forms of density dependence of symmetry energy corresponding to different values of γ'. The predictions made by the *ab-* initio microscopic calculations prescribed different forms of nuclear equation of state at sub-supra saturation densities [341–343]. Moreover, in many studies, authors have predicted symmetry energy to increase continuously at all densities [46]. However, some studies [46] advocated that the symmetry energy first increases to a certain value and then decreases at supra-saturation densities.

5.3 Different observables used to pin down the density dependence of symmetry energy

It is well known that one can not pin down density dependence of nuclear symmetry energy directly and therefore, various obserables have been reported in the literature to constrain its density dependent form. In the recent years, with the help of isospin sensitive observables (studied using RIB facilities), some success has been met to check the density dependence of the symmetry energy at sub-saturation density region. On the other hand, the form of the density dependence of symmetry energy at supra-saturation density region is still uncertain. Broadly, different observables used to constrain the density dependence of symmetry energy are classified into two categories: viz observables at sub-saturation and observables at supra-saturation density regions. Here, we will randomly review some of the attempts made in the past to constrain the density dependence of symmetry energy both at sub- and supra-saturation density regions with the help of various observables.

5.3.1 Observables in sub-saturation density region

As stated earlier, the behavior of density dependence of nuclear symmetry energy at sub-saturation density region has been constrained by studying different observables such as isospin diffusion [126, 317], isospin fractionation [322], isobaric ratios of various species [323], fragment yields [46], single and double neutron-proton (n/p) ratios [318–320, 324], isoscaling [46] etc. These observables have been used extensively to constrain the density dependence of symmetry energy below the saturation density.

Experimentally, only very limited data (mostly from the reactions with stable beams at intermediate energies) have so far been available for the comparison with theoretical calculations and these comparisons [46] help to provide valuable information about the density dependence of symmetry energy at sub-saturation densities. For example, Famiano *et al.* [320] compared experimental measurements for double neutron-proton (n/p) ratio with BUU97 calculations [344] for the reactions of $^{112,124}_{50}$Sn + $^{112,124}_{50}$Sn at 50 MeV/nucleon (at NSCL/MSU) and put forward a density dependence of the form E_{sym} = 32 $(\rho/\rho_0)^{\gamma'}$ with $\gamma' = 0.5$ (where 32 MeV is the value of symmetry energy at normal nuclear matter density). Tsang *et al.* [333] performed the calculations for isospin diffusion and n/p double ratio and concluded value of γ' between 0.4 and 1.05. Another study was performed by Zhang *et al.* [127] to calculate the n/p yields for the reactions of $^{124}_{50}$Sn + $^{112}_{50}$Sn at 50 MeV/nucleon using ImQMD model [127] and the results were compared with experimental data of Famiano *et al.* [320] for $\gamma' = 0.5$ and 2. The value $\gamma' = 0.5$ could explain the experimental results very nicely. On the other hand, comparison of the data with Constrained Molecular Dynamics (COMD) calculations favored stiffer behavior (γ' = 2) of symmetry energy [345]. Also, the IQMD model was used in this direction by Kumar *et al.* [319]. They studied the effect of density dependence of symmetry energy on single and double n/p ratios and kinetic energy spectra of neutrons and protons for the reactions of $^{112}_{50}$Sn + $^{112}_{50}$Sn, $^{124}_{50}$Sn + $^{124}_{50}$Sn and $^{132}_{50}$Sn + $^{132}_{50}$Sn at 50 MeV/nucleon and after comparing the results with measurements [320], favored the softer ($\gamma' = 0.5$) form of the density dependence. A similar form of the density dependence of symmetry energy was also put forward by Zhang *et al.* [235], after comparing the behavior of double n/p ratio from transversely emitted nucleons to center-of-mass energy within the framework of ImQMD code for the reactions of $^{112}_{50}$Sn + $^{112}_{50}$Sn, $^{124}_{50}$Sn + $^{124}_{50}$Sn at 50 MeV/nucleon.

Similarly, lot of studies have been performed for isospin diffusion and isoscaling [46,

332, 335]. For instance, Shetty *et al.* [332] compared the isoscaling parameter obtained from the reactions of ($^{40}_{18}$Ar, $^{40}_{20}$Ca) + $^{58}_{26}$Fe, $^{58}_{28}$Ni +($^{58}_{28}$Fe, $^{58}_{28}$Ni) and put forward symmetry energy of the form $E_{sym} = 31.6\ (\rho/\rho_0)^{\gamma'}$ with $\gamma' = 0.69$. Li *et al.* [46] compared the isospin diffusion data from the reactions of $^{124}_{50}$Sn + $^{112}_{50}$Sn at 50 MeV/nucleon with IBUU04 calculations and obtained symmetry energy of form $E_{sym} = 31.6\ (\rho/\rho_0)^{\gamma'}$ with $\gamma' = 0.69$. Chen *et al.* [335] also compared the isospin diffusion data and obtained the above form with $\gamma' = 1.05$. Also, transverse flow of IMFs for the reactions of $^{70}_{30}$Zn + $^{70}_{30}$Zn, $^{64}_{30}$Zn + $^{64}_{30}$Zn and $^{64}_{28}$Ni + $^{64}_{28}$Ni at 35 MeV/nucleon is analyzed with NIMROD-ISIS. The measured results were compared with the predictions of AMD, COMD and SMF models [346] and stiffer form of density dependence of symmetry energy was reported to provide a good agreement through out the spectra. Thus, one can conclude that a considerable success has been obtained to constrain the density-dependence of symmetry energy at sub-saturation density region.

5.3.2 Observables in supra-saturation density region

The behavior of density dependence of symmetry energy at supra-saturation density region, however, is poorly known in contrast to the behavior at sub-saturation density region because of limited high energy experiments. The different observables that are used to constrain the density dependence of symmetry energy at supra-saturation density region are π^-/π^+ ratio [326], the n/p differential collective flow [327], triton/He^3 ratio [328], K^+/K^0 ratio [329], η meson production [330], Σ^-/Σ^+ ratio [347], n-p ratio of squeezed out nucleons [46] etc. For example, Li *et al.* [46, 326] proposed π^-/π^+ ratio to be sensitive to the density dependence of nuclear symmetry energy at supra-saturation densities. At GSI, the FOPI collaboration calculated the π^-/π^+ ratio in the reactions of $^{40}_{20}$Ca + $^{40}_{20}$Ca, $^{96}_{40}$Zr + $^{96}_{40}$Zr, $^{96}_{44}$Ru + $^{96}_{44}$Ru and $^{197}_{79}$Au + $^{197}_{79}$Au at Bevalac SIS/GSI energies and compared this data with several model calculations. Interestingly, the confrontation of FOPI data [348] with one theoretical model yielded softer nature of symmetry energy [334] whereas, same data when compared with another theoretical model advocated stiffer form of symmetry energy [331].

In addition to neutron-rich nuclei, the effect of density dependence of symmetry energy is also studied using K^0/K^+ ratio for proton-rich reaction of $^{22}_{14}$Si + $^{22}_{14}$Si at 400 MeV/nucleon [349]. Also, a promising, a study has been performed by Li *et al.* [326] to probe the effect of the density dependence of symmetry energy by investigating the

K^0/K^+ ratio in the reaction of $^{132}_{50}$Sn + $^{132}_{50}$Sn at 1.4 GeV/nucleon. This study revealed a weak sensitivity towards density dependence of symmetry energy at *kaon production threshold* using UrQMD model, whereas, Ferini *et al.* [329] reported stronger sensitivity of K^0/K^+ ratio towards density dependence of symmetry energy for the central collisions of $^{197}_{79}$Au + $^{197}_{79}$Au using RBUU (Relativistic Boltzmann-Uehling-Uhlenbeck) model. Not only π^-/π^+ and K^0/K^+ ratio, Σ^-/Σ^+ ratio has also been proposed to be a better candidate to investigate the high density behavior of symmetry energy.

In another study, Yong *et al.* [349] proposed hot photon production as a probe to study the high density behavior of the symmetry energy. Similarly, a detailed study of single and double n/p ratios was performed by Kumar *et al.* [350] for the reactions of $^{112}_{50}$Sn + $^{112}_{50}$Sn and $^{124}_{50}$Sn + $^{124}_{50}$Sn at 50-600 MeV/nucleon and they found that the single n/p ratio from free nucleons (FNs) as well as light charged particles (LCPs) is sensitive to density dependence of symmetry energy, isospin asymmetry as well as to incident energy of the system. Also, Li *et al.* [318] studied the single and double n/p ratio of free nucleons for the reactions of $^{112}_{50}$Sn + $^{112}_{50}$Sn and $^{132}_{50}$Sn + $^{132}_{50}$Sn at 400 MeV/nucleon using IBUU04 model for soft and stiff forms of density dependence of symmetry energy and reported that double ratio has the same sensitivity as that of single ratio towards the density dependence of the symmetry energy. Moreover, in 2000, Li *et al.* [351] proposed neutron-proton differential flow to be sensitive towards density dependence of symmetry energy by considering the reactions of $^{132}_{50}$Sn + $^{124}_{50}$Sn at 400 MeV/nucleon within the framework of IBUU model. Further, Yong *et al.* [352] put forward neutron-to-proton differential flow as another candidate to constrain the density dependence of the symmetry energy. Recently, Puri and coworkers [284] reported the effect of density dependence of symmetry energy on the transverse flow in the Fermi-energy region. Therefore, we observed that though sensitivity of various observables towards density dependence of symmetry energy is well established at supra-saturation region, still the form of density dependence is far from being settled down. Therefore, lot of research is still going on to constrain high density behavior of symmetry energy.

Unfortunately, most of the observables are sensitive to both isospin-dependent nucleon-nucleon cross-section as well as to different forms of density dependence of symmetry energy. One is still hunting for those observables that can remove dual dependence and one can constrain the density dependence of symmetry energy. Again, it is worth mentioning that generally symmetric colliding partners have been taken in most of the studies carried

out to constrain density dependence of the symmetry energy. Therefore, in the present study, we will focus on the dynamics of asymmetric reactions and try to probe the density dependence of nuclear symmetry energy.

5.4 Results and discussions

For the present study, we simulated thousands of events for the central reactions of $^{40}_{18}$Ar + $^{64}_{29}$Cu, $^{40}_{18}$Ar + $^{108}_{47}$Ag, $^{40}_{18}$Ar + $^{197}_{79}$Au and p + $^{197}_{79}$Au at incident energies ranging between 17 MeV/nucleon and 11.5 GeV/nucleon. In terms of asymmetry parameter η, these reactions have η values = 0.23, 0.46, 0.66 and 0.98, respectively, therefore, mapping the entire asymmetry plane. All simulations are performed using soft equation of state supplemented by isospin- (and energy-) dependent cross section with 20% reduction (similarly as taken in the calculated results displayed in the Chapters 3 and 4) until stated explicitly. Before going to the results of isospin effects via nucleon-nucleon cross-section and density dependence of symmetry energy on the yield of fragments in nearly symmetric and asymmetric reactions, let us first check the sensitivity of our present results towards technical parameters at freeze-out time.

5.4.1 Effect of spatial and momentum correlations at freeze-out time

Since, we are dealing with multifragmentation, proper knowledge of the correlations among nucleons (i.e., clusterization range) is crucial as these may differ depending on the physical conditions such as excitation energy and system size of the colliding nuclei [232]. Therefore, before checking the sensitivity of fragmentation towards isospin effects, we will first check the role of different clusterization ranges on the multiplicities of various fragments. So to ascertain the dependence of our discussion on technical parameters, we display in Fig. 5.1, the final freeze-out heaviest fragment $<A_f^{max}>$ as well as multiplicities of the light charged particles LCPs ($2 \leq A_f \leq 4$) and intermediate mass fragments IMFs ($5 \leq A_f \leq 38$) at different incident energies ranging between 17 and 400 MeV/nucleon for the reactions of $^{40}_{18}$Ar + $^{64}_{29}$Cu, $^{40}_{18}$Ar + $^{108}_{47}$Ag and $^{40}_{18}$Ar + $^{197}_{79}$Au. We also display the average values of the above said quantities for clusterization ranges R_{clus} between 3 and 6 fm (solid hexagons). We clearly see that R_{clus} = 4 fm (open circles) depicts the average behavior of different clusterzation ranges used in the literature. It is worth mentioning that R_{clus}

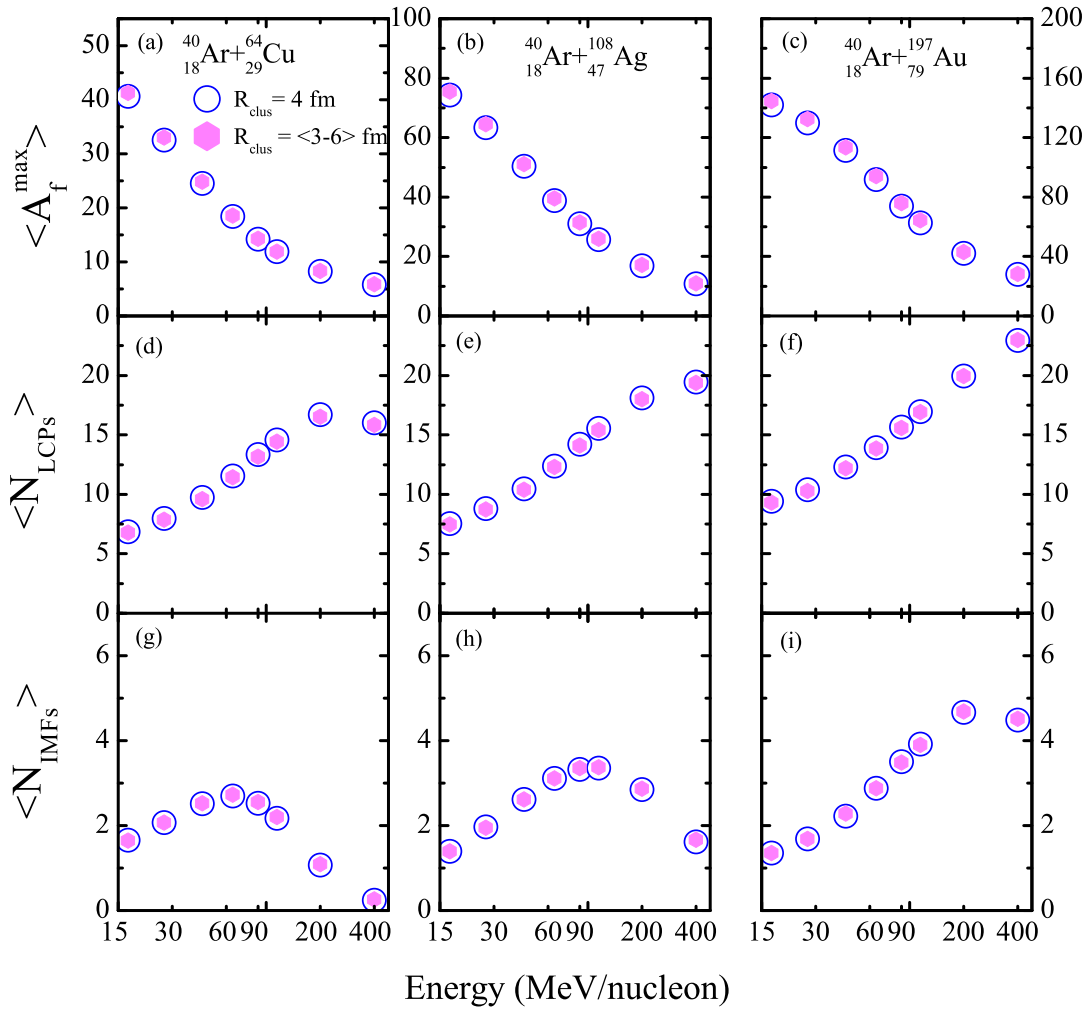

Figure 5.1: The size of heaviest fragment $<A_f^{max}>$ and multiplicities of light charged particles (LCPs) and intermediate mass fragments (IMFs) as a function of beam energy obtained in the central collisions ($\widehat{b}$ = 0 - 0.15) of $^{40}_{18}$Ar + $^{64}_{29}$Cu, $^{40}_{18}$Ar + $^{108}_{47}$Ag and $^{40}_{18}$Ar + $^{197}_{79}$Au. Open circles and solid hexagons represent the results with different values of clusterization range i.e., R$_{clus}$ = 4 fm and average of 3-6 fm, respectively.

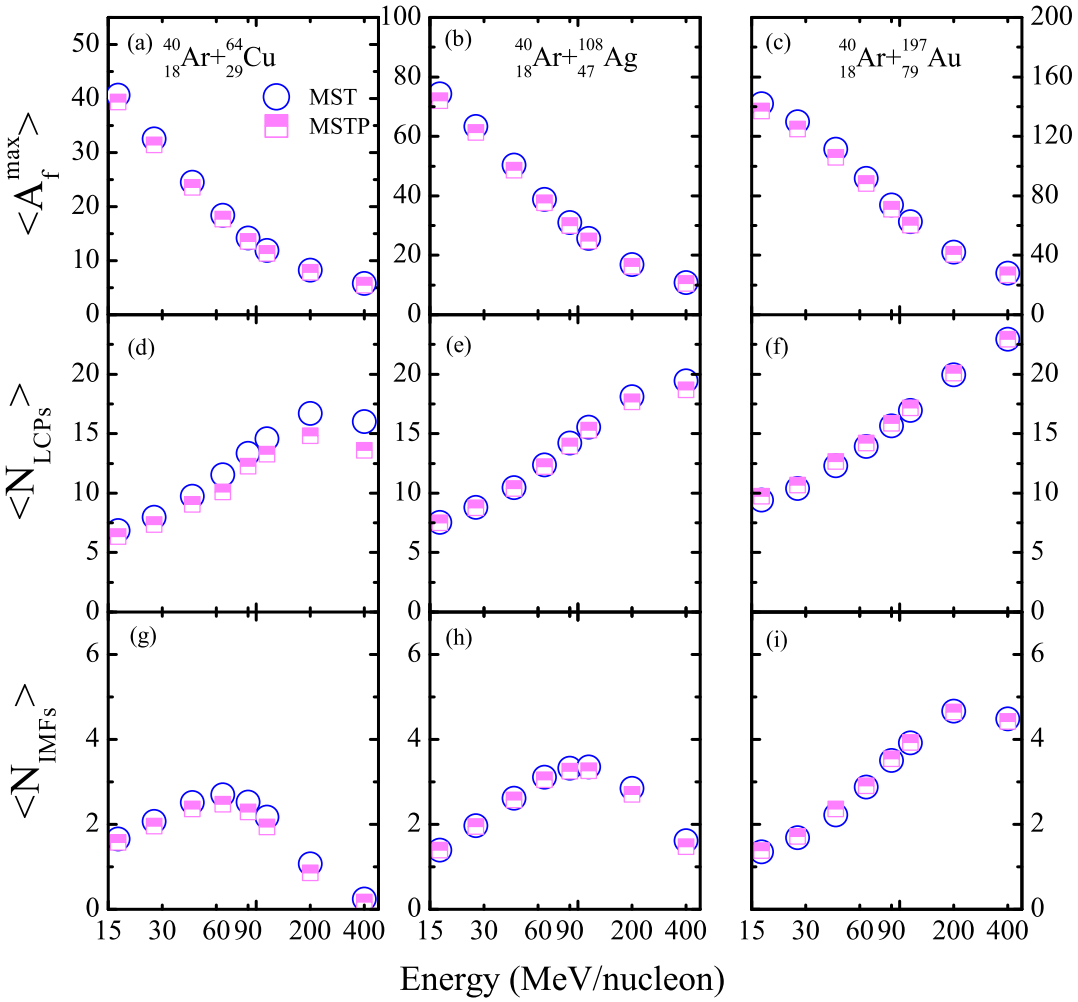

Figure 5.2: Same as Fig. 5.1, but here circles and half filled squares represent the calculations with MST and MSTP approaches, respectively.

= 3 and 6 fm has also been used in, so called, iso-MST studies [235].

Many times in the literature, additional momentum cuts are also imposed to filter out unrealistic fragments [61, 203, 236]. To investigate the influence of such additional cuts, we display in Fig. 5.2, our calculations of default MST method along with one where additional momentum cut (of 200 MeV/c) has also been imposed (labelled as MSTP). Again, we see that this additional cut is not needed in the present calculations that comprises of nearly symmetric and asymmetric reactions. From the above discussions, it is very clear that technical parameters do not affect the outcome and hence one can discuss isospin effects accurately. Let us first give a brief introduction of different nucleon-nucleon scattering cross-sections used in the literature and after that we shall investigate isospin effects via nucleon-nucleon scattering cross-section.

5.5 Different nucleon-nucleon scattering cross-sections

In the literature, various types of nucleon-nucleon (NN) cross-sections that include constant, energy-dependent, in-medium NN cross-sections have been used to study the hot and dense nuclear matter at intermediate energies [22, 24, 272, 353]. In many of the earlier studies, a constant cross-section (having magnitude lying between 20 and 55 mb) has been used to simulate heavy-ion collisions [354–356]. Even studies do exist in the literature where multifragmentation phenomenon has been studied using constant cross-section [233, 356]. Also, it is well accepted that the free NN cross-section depends strongly on the incident energy [357].

In this direction, cross-section parameterized by Cugnon *et al* [209] has been incorporated in large number of studies [22, 24, 29, 273, 284, 291, 292, 353]. At the same time, it is worth mentioning that the cross-section can change by the nuclear medium [358, 359]. Due to much pronounced effect of Pauli-principle at low incident energies (about 96% of collisions blocked) than at higher incident energies (where Pauli-principle blocks only 4% collisions at 2 GeV/nucleon), it is necessary to take care of the proper in-medium effects at low incident energies. Faessler and collaborators were the first to take initiative and they derived the complete in-medium cross-section using the G-matrix calculations [188, 360]. The G-matrix calculations resulted a considerable reduction in the NN cross-section in the medium.

Further, it is worth mentioning that calculations of G-matrix for the in-medium NN cross-section are complicated, therefore, a constant scaling factor or density-dependent reduced (DDR) cross-section has been preferred to take care of the in-medium effects. Following this, various studies on transverse and elliptic flow, fragmentation etc. are carried out using the density dependence scaling in the free energy-dependent nucleon-nucleon cross-section [302, 305, 308, 348, 353]

5.5.1 Isospin effects via nucleon-nucleon cross-section

As mentioned above, isospin effects are often discussed in terms of isospin dependence of the binary nucleon-nucleon cross-section as well as density dependence of the symmetry energy. However, often one encounters the problem of dual dependence on both these parameters.

In Fig. 5.3, we study the role of scattering nucleon-nucleon cross-sections in the fragmentation of above asymmetric colliding systems. Here, we extend our calculations to extreme asymmetric reaction of p + $^{197}_{79}$Au at incident energies between 17 MeV/nucleon and 11.5 GeV/nucleon. We took three cross-sections namely, isospin-dependent cross-section (σ_{NN}), isospin independent cross-section (σ_{noniso}) and density-dependent reduced cross-section (σ_{DDR}). The density-dependent reduced (DDR) cross section involves a reduction factor depending upon the density and reads as $\sigma_{DDR} = (1 - 0.2\ \rho/\rho_0)\ \sigma_{NN}^{free}$, where σ_{NN}^{free} is isospin-dependent nucleon-nucleon cross-section in free space. It is worth mentioning that the density-dependent nucleon-nucleon cross-section has been advocated in large number of studies as well [56, 269, 271, 272]. Very interestingly, fragmentation pattern in terms of heaviest fragment $<A_f^{max}>$, light charged particles (LCPs) and intermediate mass fragments (IMFs) is completely insensitive towards different nucleon-nucleon cross-sections. We have also checked the number of binary collisions, experienced by the nucleons in each case and found that different cross sections alter the collision number by about 10% on the average, therefore, results in insignificant effect. It is worth mentioning that recently Puri and coworker showed a complete insensitiveness of entropy production towards isospin dependence of the nucleon-nucleon cross-section [361]. Let us now study isospin effects via density dependence of symmetry energy.

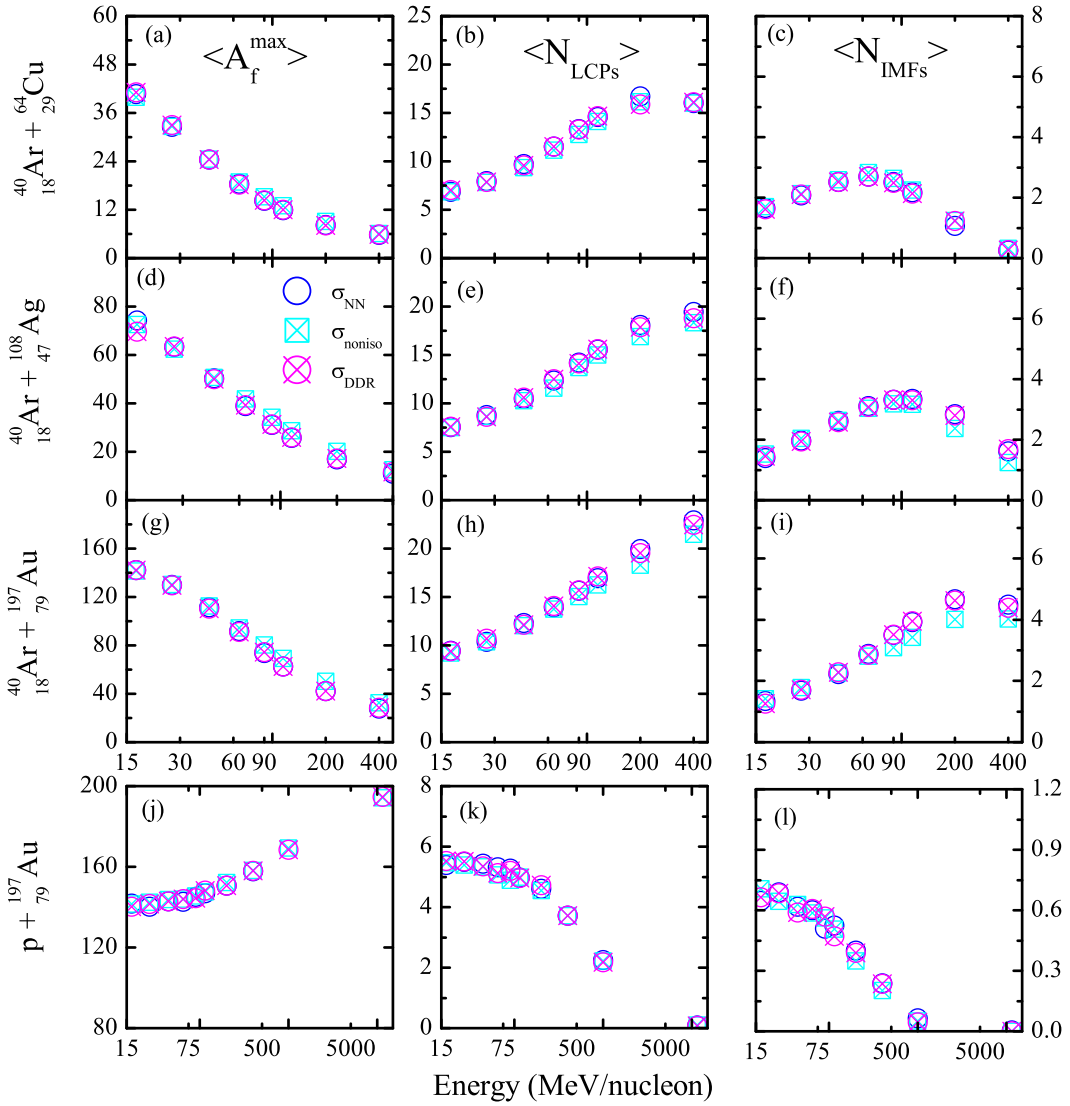

Figure 5.3: The size of heaviest fragment $<A_f^{max}>$ and multiplicities of light charged particles (LCPs) and intermediate mass fragments (IMFs) as a function of beam energy in the central collisions ($\widehat{b}$ = 0 - 0.15) of $^{40}_{18}$Ar + $^{64}_{29}$Cu, $^{40}_{18}$Ar + $^{108}_{47}$Ag, $^{40}_{18}$Ar + $^{197}_{79}$Au and p + $^{197}_{79}$Au. Here, different symbols represent various NN scattering cross sections. Circles, crossed squares and crossed circles represent the results using isospin-dependent, isospin independent and density-dependent reduced (DDR) cross sections, respectively. The last two points in the bottom panels (i.e., for p + $^{197}_{79}$Au) are at 1 GeV/nucleon and 11.5 GeV/nucleon.

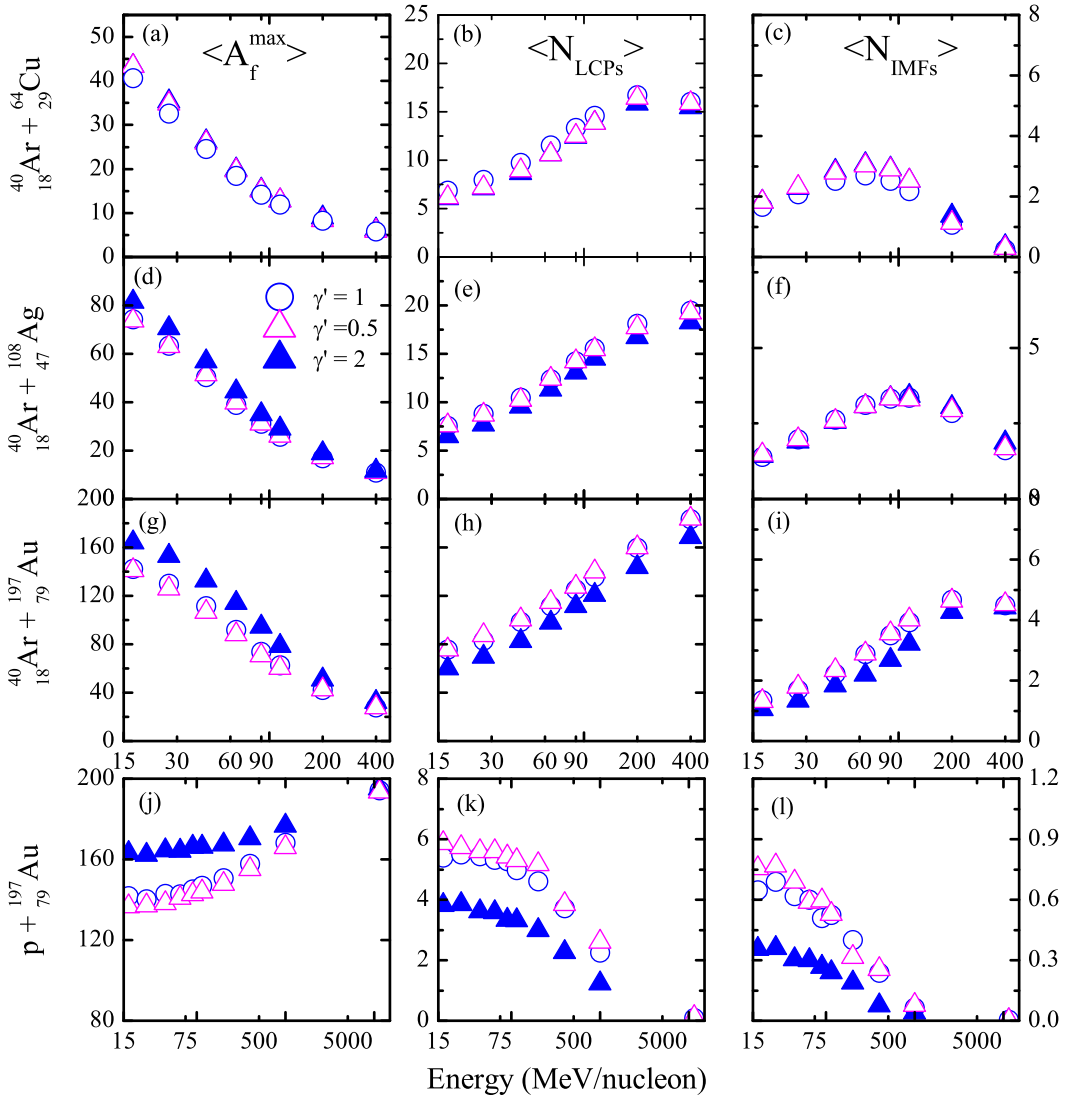

Figure 5.4: Same as Fig. 5.3, but here different symbols represent different forms of density dependence of symmetry energy. Solid (open) triangles represent the results using stiff, γ' = 2 (soft, $\gamma' = 0.5$) symmetry energy, whereas, circles represent our default calculations ($\gamma' = 1$).

5.5.2 Isospin effects via density dependence of symmetry energy

The sensitivity of fragmentation towards second isospin effect, namely, different density dependencies of symmetry energy is shown in Fig. 5.4. In addition to our default symmetry energy ($\gamma'= 1$), we also took density dependence of symmetry energy with $\gamma'=$ 0.5 (soft) and $\gamma'= 2$ (stiff). Very interestingly, we notice that the effect of different density dependence of symmetry energy increases as one moves towards highly asymmetric reactions. The symmetric reactions, in accordance with previous investigations [56, 361, 362], do not yield different results whereas, fragmentation in highly asymmetric reactions such as p + $^{197}_{79}$Au has huge sensitivity towards different forms of symmetry energy though, it is completely insensitive towards isospin dependence of the binary nucleon-nucleon cross-section. Note that most of the previous studies [46, 284, 317–321, 325, 327–329, 331–334, 348] took symmetric reactions only. We show here, for the first time, that the highly asymmetric reactions do not have dual dependence, therefore, pose excellent candidate to pin down the density dependence of the symmetry energy. As noted, the stiff symmetry energy (solid triangles) leads to bigger $<A_f^{max}>$ compared to the one obtained with linear dependence or soft symmetry energy (circles or open triangles). This happens because of the extra repulsion provided by the stiffer symmetry energy ($\propto \rho^2$) leading to reduced binary nucleon-nucleon collisions. One, therefore, observes a bigger $<A_f^{max}>$ compared to that obtained with default calculations ($\gamma'= 1$). Similar trends are also seen in transverse momentum where stiff symmetry energies (being more repulsive) lead to enhanced transverse momentum compared to softer one [284]. The inverse is true for the production of various mass fragments where higher yields of lighter and intermediate mass fragments are observed with soft symmetry energy. We find that for less asymmetric reaction of $^{40}_{18}$Ar + $^{64}_{29}$Cu, one gets slightly higher yield with stiff symmetry energy compared to default calculations which is opposite to that observed in case of highly asymmetric reactions of $^{40}_{18}$Ar + $^{197}_{79}$Au (compare circles and solid triangles). This happens because of significant compression in less asymmetric reaction of $^{40}_{18}$Ar + $^{64}_{29}$Cu which, in turn, breaks the system into various small/medium sized fragments. On incorporating stiffer symmetry potential, the yield of intermediate mass fragments increases due to extra repulsion generated by the stiffer form. On the other hand, due to reduced compression in highly asymmetric reactions, one observes higher yield with softer form of the symmetry energy (less repulsive) compared to stiffer one as now softer form of the symmetry energy breaks the system into

various fragments. Similar findings were also reported in Ref. [56] where isospin effects in fragmentation of $^{76}_{30}$Zn + $^{40}_{18}$Ar were studied within the framework of IQMD model. From the above analysis, it is very encouraging to note that highly asymmetric reactions are excellent candidates to pin down the density dependence of symmetry energy.

Till now in this study, we have only calculated the yield of fragments and found that in asymmetric reactions, yield of fragments can help to probe the density dependence of symmetry energy. Obviously, one is interested to look for other properties which help to validate our findings. In this direction, we next study the isospin effects on momentum (p_T) spectra of various fragments.

5.5.3 Isospin effects via nucleon-nucleon cross-section and density dependence of symmetry energy on momentum spectra

To further strengthen our point, we also investigate the transverse momentum spectra (p_T spectra) of free nucleons as well as of various mass fragments using different cross-sections as used in Fig. 5.3 as well as different density-dependent forms of symmetry energy as taken in Fig. 4.4 for the reaction of p + $^{197}_{79}$Au at 17 and 200 MeV/nucleon. The results are displayed in Fig. 5.5 (see left and right panels for different cross-sections and different density-dependent forms of symmetry energy, respectively). The main reason of choosing this reaction is that we are interested in studying isospin effects on different observables in extreme asymmetric reactions. Very interestingly, again we see that the p_T spectra is completely insensitive towards isospin dependence of the cross-section but is highly sensitive towards soft and stiff forms of the symmetry energy. This further leads to the conclusion that asymmetric reactions are better candidates to pin down the density dependence of symmetry energy as they remove the dual dependence behavior (as discussed earlier).

5.5.4 Soft and stiff form of symmetry energy: comparison with data in asymmetric reactions

Finally, we compare our results with experimental findings in order to pin down suitable form of density dependence of symmetry energy advocated by multifragmentation of asymmetric heavy-ion collisions. In Fig. 5.6, we display the size of heaviest fragment $<A_f^{max}>$ and multiplicities of light charged particles (LCPs) and the intermediate mass

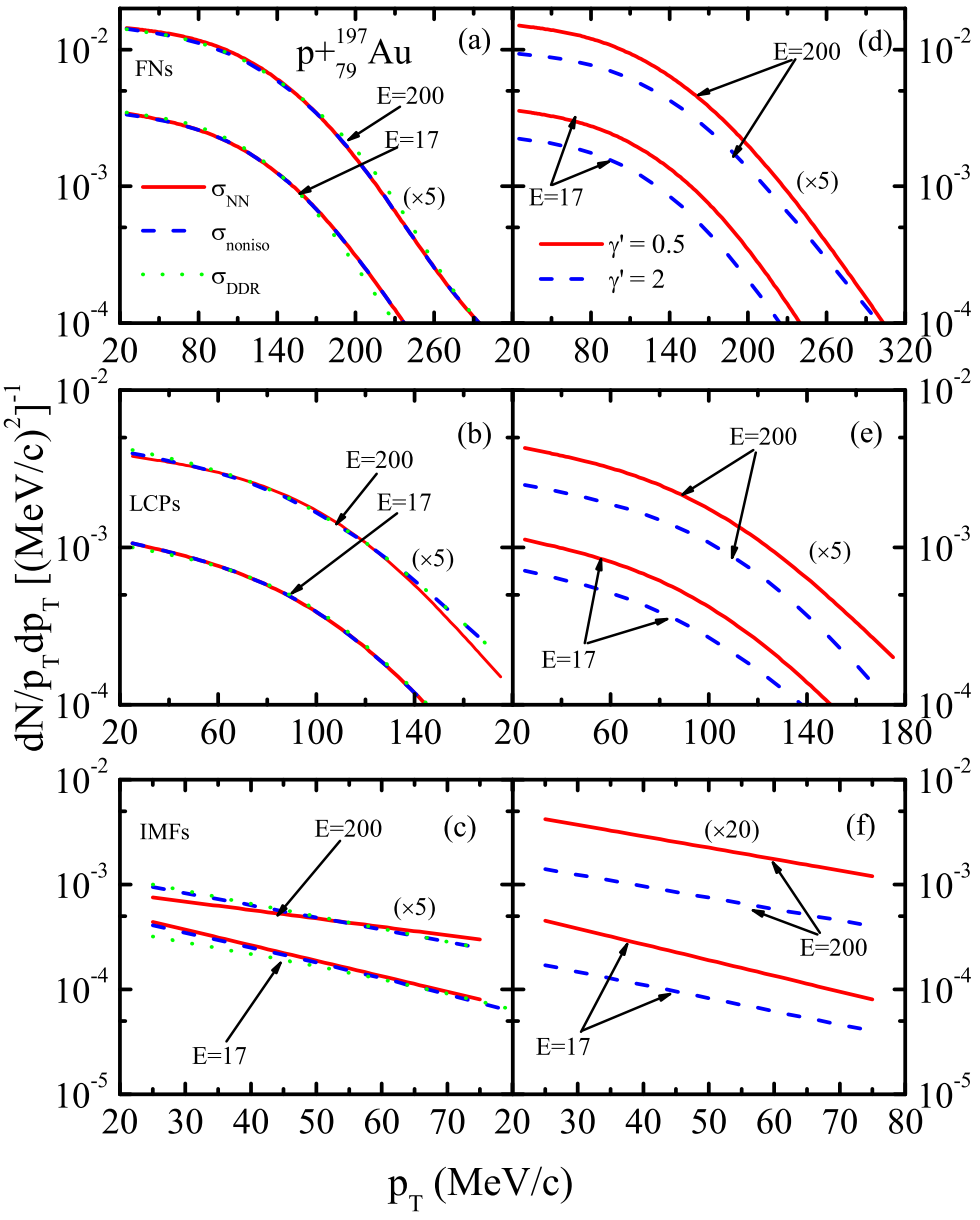

Figure 5.5: The p_T spectra for central p + $^{197}_{79}$Au collisions at two different incident energies of 17 and 200 MeV/nucleon. In the left panels, we display the results of different nucleon-nucleon cross-sections. The solid, dashed and dotted lines represent the calculations with isospin-dependent, isospin independent and density-dependent reduced cross-sections, respectively. In the right panels, we take two density dependencies of symmetry energy i.e., soft ($\gamma' = 0.5$) and stiff ($\gamma' = 2$) and results are shown by solid and dashed lines, respectively. Also, at E = 200 MeV/nucleon, results of p_T spectra have been scaled by different factors as shown in the figure (in brackets).

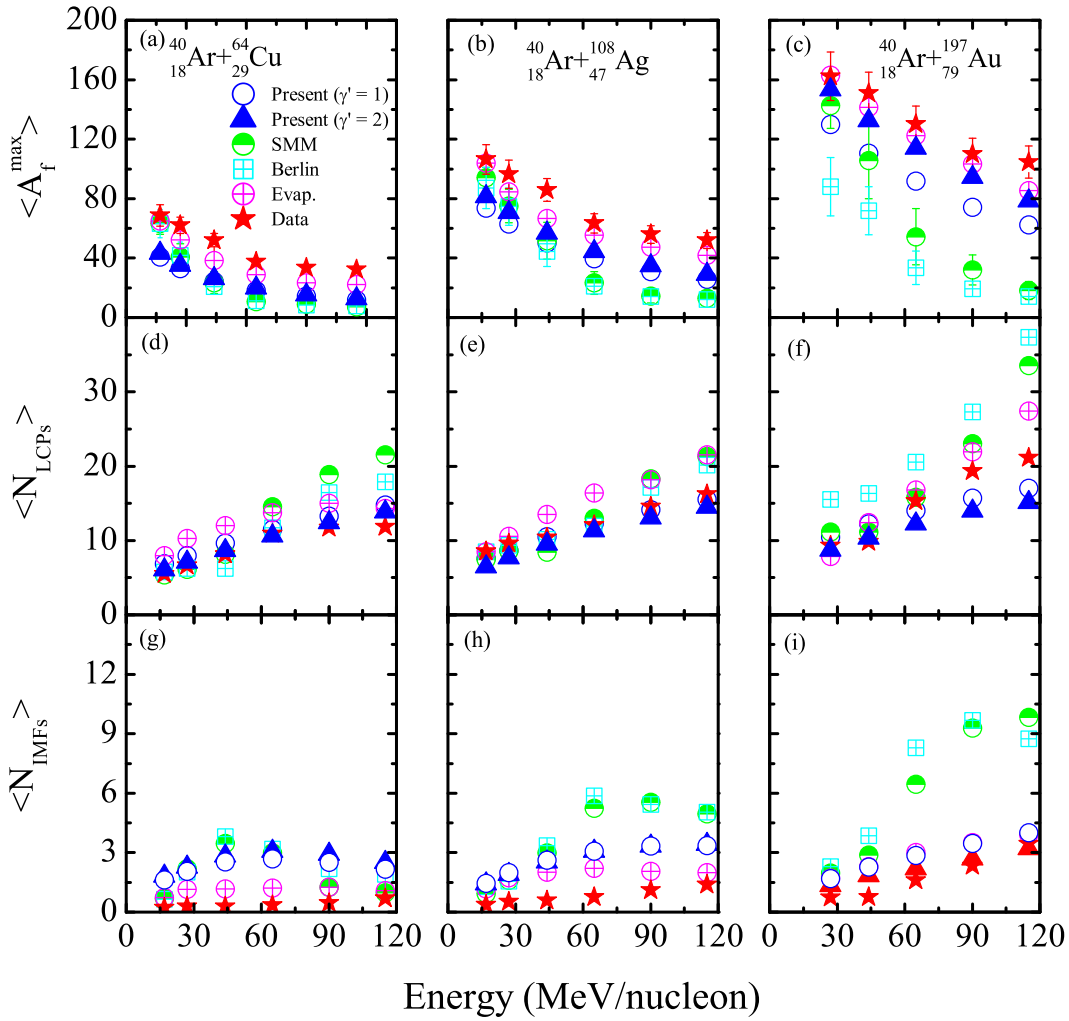

Figure 5.6: The size of heaviest fragment $<A_f^{max}>$ (top panel), multiplicities of light charged particles $<N_{LCPs}>$ (middle) and intermediate mass fragments $<N_{IMFs}>$ (bottom) as a function of incident energy for the central collisions of $^{40}_{18}$Ar + $^{64}_{29}$Cu, $^{40}_{18}$Ar + $^{108}_{47}$Ag and $^{40}_{18}$Ar + $^{197}_{79}$Au. Open circles (solid triangles) represent our present calculations using $\gamma' = 1$ ($\gamma' = 2$). Experimental data and other model calculations are taken from Ref. [97].

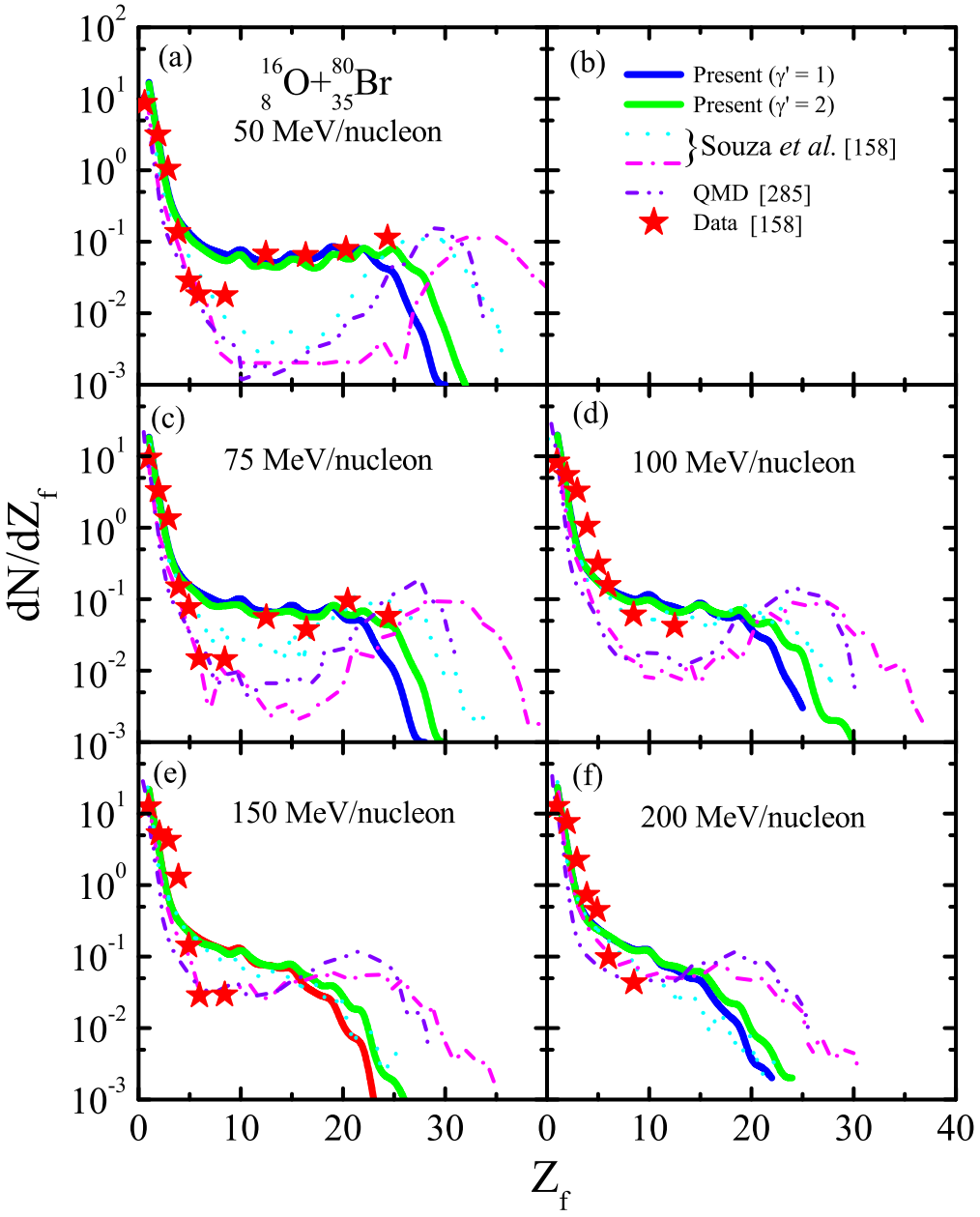

Figure 5.7: The charge distributions for the reaction of $^{16}_{8}O + ^{80}_{35}Br$ at incident energies between 50 and 200 MeV/nucleon. Solid (dashed) lines represent our present calculations using $\gamma' = 1$ ($\gamma' = 2$). Stars represent experimental data and is extracted from Ref. [158]. The results of previous theoretical attempts [158] are also displayed for comparison

fragments (IMFs) as a function beam energy. It should be noted that choice of central collisions and range of IMFs ($5 \leq A_f \leq 38$) has been done as per measurements [97]. Note that measurements [97] (displayed by stars) are done up to the beam energy of 115 MeV/nucleon only. The results of previous attempts using SMM (half filled circles), Berlin (crossed squares) and Evaporation (crossed circles) models are also shown. In Fig. 5.6, we display the results with different forms of density dependence of symmetry energy so as to give the best possible approximation of the nuclear symmetry energy which is of great debate these days. From the figure, we find that our calculated results (using IQMD model) with stiffer symmetry energy are closer to experimental data compared to softer one. This conclusion agrees well with various other studies [46, 331, 346, 363, 364] where stiffer form of symmetry energy has been proposed at supra-saturation density region.

To further strengthen our view point, we compare in Fig. 5.7, our calculated results for the charge distributions with the measured ones [158] for asymmetric reactions of $^{16}_{8}$O + $^{80}_{35}$Br at central colliding geometry at five different incident energies between 50 and 200 MeV/nucleon. The results of other models [158] are also shown for comparison. We again find that in most of the cases our calculated results using stiffer symmetry energy are closer to measured ones in the Fermi-energy domain. Thus, we can conclude that multifragmentation in highly asymmetric colliding systems can possibly be explained well with stiffer form of density dependence of symmetry energy. Since, these studies are very limited in number therefore, further studies are needed to strictly constraint the density dependence of symmetry energy in supra-saturation density region.

5.6 Summary

Summarizing, we presented our analysis of the effect of isospin dependence of nucleon-nucleon cross-section as well as different density dependencies of symmetry energy on fragmentation of various mass asymmetric reactions. Very interestingly, we found that isospin dependence of nucleon-nucleon cross-section do not influence the yield of fragments and their transverse momentum spectra in all reactions. However, different density dependencies of symmetry energy significantly alter the dynamics as asymmetry of the reaction increases. For highly asymmetric reactions such as p + $^{197}_{79}$Au, one can see significant difference in the results with soft and stiff forms of symmetry energies which, on the other hand, remain mute towards isospin dependence of cross-section. In our opinion,

highly asymmetric reactions pose powerful candidates for pining down the density dependence of symmetry energy. Further, comparison of calculated results (taking different values of γ') with experimental measurements in some asymmetric reactions favors stiffer form of density dependence of symmetry energy.